

## Effect of low-temperature oxidation on the properties of TiVN/VN multilayer coatings

Merve ERTAŞ USLU<sup>1,2</sup> , Özge DOĞAN<sup>3</sup> , Leyla ÇOLAKEROL ARSLAN<sup>1,3,\*</sup> 

<sup>1</sup>Department of Physics, Gebze Technical University, Kocaeli, Turkey

<sup>2</sup>Faculty of Engineering and Natural Sciences, Sabancı University, İstanbul, Turkey

<sup>3</sup>Nanotechnology Institute, Gebze Technical University, Kocaeli, Turkey

Received: 26.10.2018

Accepted/Published Online: 13.02.2019

Final Version: ..201

**Abstract:** An extensive study of the surface oxidation process on the properties of TiVN/VN multilayer coatings deposited by RF magnetron sputtering on Mg alloys was performed. TiVN/VN multilayer coatings with a total thickness of 660 nm and different layer numbers of 5, 11, and 33 were oxidized by annealing at 450K under partial oxygen pressure. Electronic, mechanical, and tribological properties of these coatings were characterized by X-ray photoelectron spectroscopy (XPS), scanning electron microscope, nanoindentation measurements, and scratch tester. The experimental results showed that the oxidation of TiVN/VN multilayer coatings leads to better performance in terms of surface roughness, hardness, and wear. The hardness of the coating increased significantly (up to 1400 HV) with the oxidation of the surface due to the release of stresses between each layer after in situ annealing. The decline of the friction coefficient after oxidation can be attributed to the formation of a self-lubricating  $V_2O_5$  layer on the surface, the presence of which was confirmed by XPS. The findings in this work reveal a new technique for applying a better thin film coating for industrial applications of Mg alloys.

**Key words:** Multilayer nitride coatings, TiVN/VN, surface oxidation, tribological properties

### 1. Introduction

Mg alloys have a wide range of applications in automotive and aerospace industries due to their light weight, good castability, and high stiffness. For widespread use of magnesium alloys, it is necessary to improve their strength and toughness. Coating magnesium alloy surfaces is one possible technique for increasing their mechanical properties. Transition metal nitrides like TiN, VN, AlN, CrN, and their ternary alloys have been successfully used as a wear protective coating material for Mg alloys [1–4]. Due to its well-known high hardness and low adhesion tendency, TiN is the most frequent coating material for engineering tools and electric components. However, the low oxidation resistance of Ti-based coatings at elevated temperatures leads to degradation of the tribological effectiveness of these coatings [5].

Recent studies have shown that the multilayer coatings obtained from different combinations of nitrides have higher hardness and sliding wear resistance compared to a single layer form [6–8]. Numerous studies performed on (Ti,V)N/VN and (Ti,Al)N/VN nanoscale multilayer coatings have indicated that the wear performance and hardness were significantly improved, depending on the chemical composition [9–13]. The hardness of a multilayer coating depends on the period and composition of layers and the structure of the

\*Correspondence: lcolakerol@gtu.edu.tr

interface between each layer. Wear resistance, on the other hand, is directly affected by surface structural properties such as surface roughness, porosity, and surface finish quality. VN oxidizes easily to form Magnéli phases or highly oxidized vanadium oxides which are thermodynamically stable under ambient conditions [14,15]. The beneficial influence of Magnéli phases on the tribological behavior of V-containing nitride coatings has already been reported [14–17]. Among these phases,  $V_2O_5$  gives rise to self-lubrication of the surface layer [6,18]. Evidence for the formation of lubricating oxides on VN has come from X-ray diffraction (XRD) [14] and X-ray photoelectron spectroscopy (XPS) studies [19], which have revealed that oxide layers containing various vanadium state structures were formed on the entire surface depending on the annealing temperature and oxygen dose. All of these studies have demonstrated that formation of lubricious vanadium oxides at elevated temperatures ( $>500$  °C) leads to lower friction coefficient. Similarly, the friction coefficient of directly grown  $V_2O_5$  films improved significantly at elevated temperatures [20]. However, magnesium alloys have relatively poor mechanical properties at such high temperatures. The poor heat resistance of Mg alloys is the biggest obstacle for forming a lubricating vanadium oxide layer at elevated temperatures on these alloys. Therefore, we have explored the formation of an oxide layer at low temperatures to improve the wear performance of nitride coatings.

The goal of this study was to increase the wear resistance and hardness of AZ91D Mg alloys by forming TiVN/VN multilayer coatings using RF magnetron sputtering. High-quality films can be produced by RF sputtering because the reaction rate can be controlled easily and impurity levels are low. We investigated the effect of in situ oxidation at low temperature on the mechanical properties of TiVN/VN multilayer thin film coatings. This study provides a better understanding of the formation of a vanadium oxide layer at low temperatures and the impact of this lubricious oxide layer on the mechanical properties of V-containing multilayer coatings.

## 2. Experimental techniques

Thin multilayer TiVN/VN films were deposited on commercially purchased AZ91D Mg alloys using a RF magnetron sputtering system with a base pressure greater than  $1 \times 10^{-9}$  mBar. Initially, a polishing process was applied on AZ91D Mg alloy substrates. Next, the samples were ground on a flat rotating grinder with 800-, 1200-, and 2400-grit emery papers. To prevent abrasive particles from being transferred to finer-grit paper disks, the samples were cleaned with isopropyl alcohol in an ultrasonic bath after each cycle. Subsequently, they were polished with a 3- and 1- $\mu$ m diamond suspension for 30 min to eliminate the surface scratches. Before being placed into a vacuum chamber, the polished samples were cleaned with isopropyl alcohol in an ultrasonic bath and dried with nitrogen.

TiVN/VN multilayer thin film coatings were prepared using high-purity cylindrical Ti (99.9%) and V (99.9%) targets. An ultrahigh purity argon and nitrogen gas mixture with the optimum Ar/N<sub>2</sub> gas flow ratio of 1/2 was used for the development of coatings. Before the deposition of each film, the targets were presputtered in a pure argon atmosphere for 10 min in order to remove the contaminants from the target surfaces. The TiVN/VN films with a thickness of approximately 660 nm were deposited by applying 100 W RF plasma power without sample bias at a total pressure of  $1.9 \times 10^{-3}$  mBar at room temperature. The deposition rates were calibrated by X-ray reflectivity using the single-layer TiVN and VN thin films. The thickness of individual TiVN and VN layers was controlled by alternately switching the time for shutters to form the sequential TiVN/VN multilayers. During this process, the number of layers varied (5, 11, and 33), with VN being the top layer. The

oxidation process was performed without removing the samples from the vacuum environment. Oxygen was dosed in the UHV system via a leak valve and the oxygen exposure is given in Langmuir (L),  $1 \text{ L} = 1 \times 10^6$  Torr s. TiVN/VN coated surfaces were oxidized at a temperature of approximately 450 K for exposures of  $5 \times 10^4$  L oxygen.

XPS, scanning electron microscopy (SEM), and atomic force microscopy (AFM) techniques were applied to examine the composition and surface quality of the coatings. The samples were analyzed with XPS using an Al  $K\alpha$  X-ray source and a hemispherical electron analyzer (Phoibos 100, SPECS GmbH, Berlin, Germany). Spectra were calibrated using the Au  $4f_{7/2}$  signal from a clean gold foil ( $E_B 4f_{7/2} = 84.0$  eV). After the completion of film growth, XPS spectra were taken before and after the oxidation process without removing the samples from the vacuum chamber. In this manner, we confirmed that there was no other surface contamination. Surface morphology and roughness of the coated films were examined by SEM and AFM, respectively. Mechanical and tribological properties of the coatings were investigated by nanoindentation and scratch tester. Nanoindentation was performed with a continuous stiffness measurement process indentation tester (CSM Instruments, Needham, MA, USA) attached to evaluate the hardness and elastic modulus of coatings. Six separate indentations were performed on each sample with a Rockwell diamond indenter up to a maximum depth of 200 nm. The scratch was formed on the coating surface using a diamond ball with a thickness of 200  $\mu\text{m}$  along the 6-mm line and applying progressive load up to 2 N in order to measure the wear resistance of the coatings. Obtained scratch tracks were examined under an optical microscope.

### 3. Results

The chemical states of TiVN/VN multilayer coatings were investigated by XPS studies. Figure 1 shows the (a) V  $2p$  and (b) N  $1s$  core level spectra and fitted curves of TiVN/VN multilayer coating before the oxidation process. O  $1s$  core level peak is also included in the V  $2p$  region. The curves were deconvoluted using the Voigt curve fit after subtracting Shirley-type background in order to extract the chemical bonding energies. The XPS spectrum for V  $2p_{3/2}$  region of the initial TiVN/VN surface can be deconvoluted into 2 main peaks at 513.7 and 515.5 eV, corresponding to the reported binding energy for bulk VN phase and VN satellite, respectively [19,21]. The broader high energy component can also be associated with the  $V^{+3}$  oxidation state; however, no peak was observed in the O  $1s$  region [11,22]. For the N  $1s$  spectrum in the TiVN/VN coating (Figure 1b), the response comes from (Ti,V)-N bonds in the TiVN, as evidenced by a peak at the binding energy of 397.3 eV. The broad contribution, leading to an asymmetric envelope line shape, can be related to X-ray line profile due to an unmonochromatized Al anode.

V  $2p$  and N  $1s$  XPS spectra of the TiVN/VN surface after the oxidation process performed by  $O_2$  dosing at 450 K for 12 hours for exposures of  $5 \times 10^4$  L oxygen are also presented in Figure 1. As the coating was exposed to  $O_2$ , there were 2 noticeable changes: an obvious peak corresponding to O  $1s$  emerged and the line shapes of V  $2p$  and N  $1s$  spectra changed slightly. In general, V  $2p$  and N  $1s$  shifted about 0.2 eV to a lower binding energy, indicating the variation of work function with the formation of the oxide layer on the surface. The V  $2p_{3/2}$  spectrum can be deconvoluted into 3 components at binding energies of 513.5, 515.3, and 517.2 eV. Low binding energy peaks at 513.5 and 515.5 eV correspond to VN and VN satellite. The peak appearing at 517.2 eV with 1.5 eV FWHM originates from the higher state of the oxidized V-oxide compound due to the formation of  $V_2O_5$  [23,24]. Fateh et al. reported that the  $V_2O_5$  phase was obtained from films deposited on Si from V targets using magnetron sputtering above 100 °C [25]. On the other hand, studies on V-containing

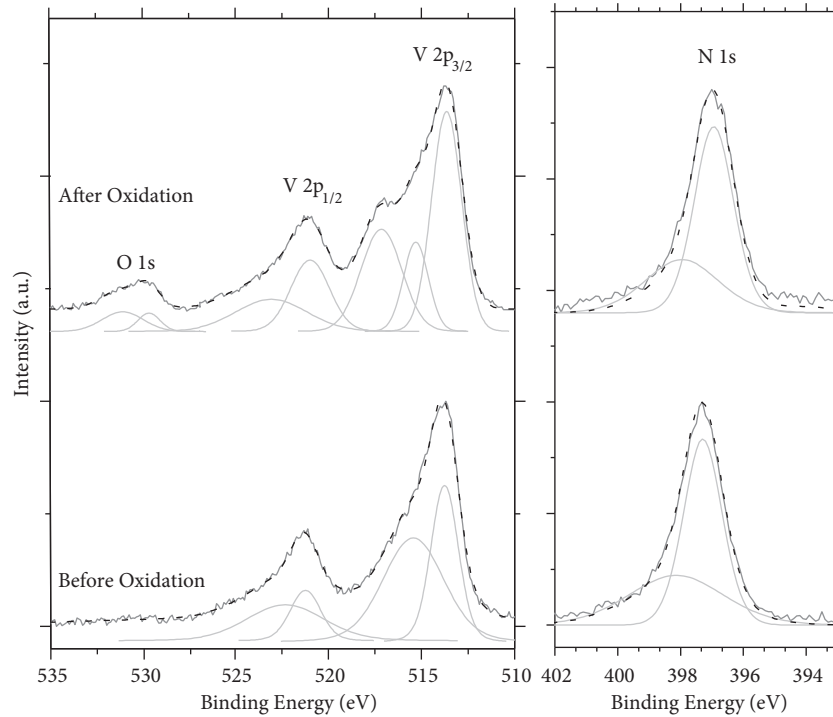
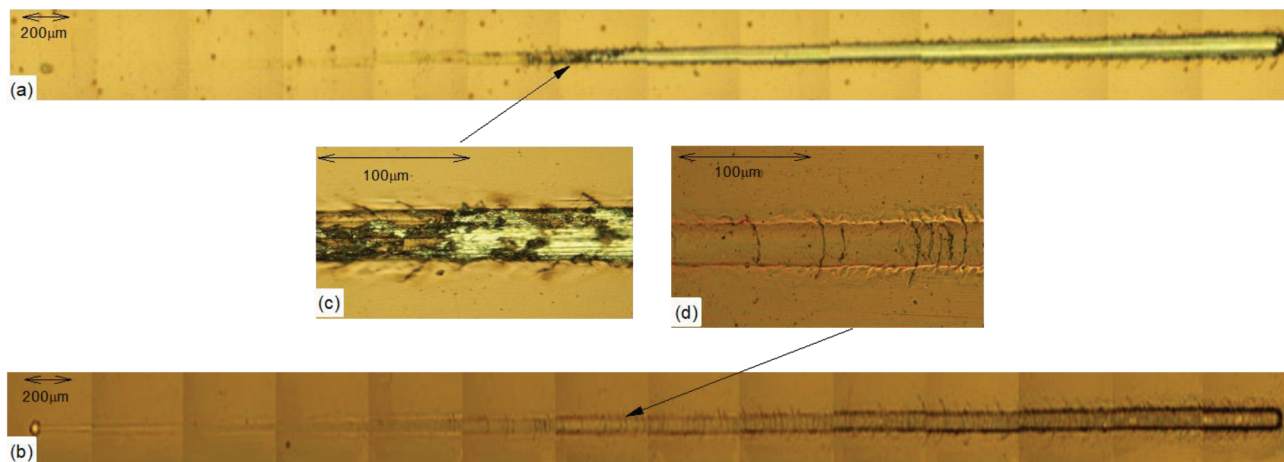


**Figure 1.** XPS spectra showing the V  $2p$ , O  $1s$ , and N  $1s$  regions of sequential 11 layers TiVN/VN coatings before and after the oxidation process.

nitrides indicated a considerable reduction of the friction coefficient of these films after heating above  $500\text{ }^{\circ}\text{C}$  under atmospheric conditions, due to the formation and softening of  $\text{V}_2\text{O}_5$  Magnéli phases [26,27]. Since annealing was performed in situ under partial oxygen pressure, the lack of residual gases might have led to the formation of a single-phase oxide layer on the surface at such low temperatures. The O  $1s$  region of the spectrum can be properly fit with 2 symmetrical peaks at  $529.7\text{ eV}$  and  $531.2\text{ eV}$ . The O  $1s$  peak at the lower binding energy has been attributed to N–O bonding. The second oxygen component positioned at  $531.2\text{ eV}$  is associated with  $\text{VO}_x$ , which is consistent with the V  $2p$  results. The oxidation of VN observed in V  $2p$  spectra is also consistent with the changes observed in N  $1s$  spectra. The higher intensity of the broader peak indicates the formation of vanadium oxynitride  $\text{VO}_x\text{N}_y$ .

Progressive load scratch tests were performed to study the effect of the oxidation process on the wear resistance and adhesion strength of TiVN/VN multilayer coatings. Scratch tracks of the oxidized and unoxidized coatings are shown in Figures 2a and 2b, while increased magnifications of the cohesive failure mode are depicted in Figures 2c and 2d, respectively. Due to limitations in the acoustic emission sensitivity, the critical load associated with the initiation of microcracks and cohesive failure could only be detected by the optical microscopy micrograph of the residual scratch track. The indenter created initial deformation on the unoxidized TiVN/VN coating at a load of  $0.55\text{ N}$ . As the load was progressively increased to  $0.9\text{ N}$ , delamination of the coating started to take place on the coating surface. After the oxidation process, transverse semicircular tracks initially formed in the groove of a scratch tester at loads of approximately  $0.66\text{ N}$ . Oxidized coating showed the first sign of a lateral crack at a load of  $1\text{ N}$  as revealed by the dark zones at the edges of the track, and extensive lateral cracking was observed starting with loads of approximately  $1.8\text{ N}$ . However, the coating maintained its adhesion to the Mg alloy throughout the test. It exhibited no sign of delamination until the end of the

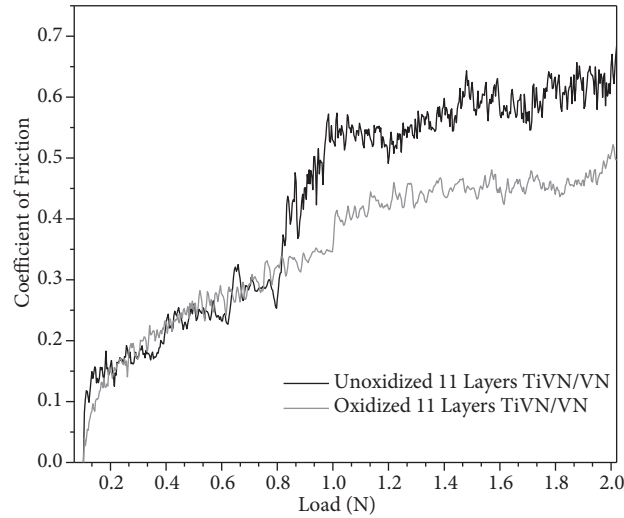
test. Comparison of critical loads showed that oxidized coating exhibited a greater level of adhesion than the unoxidized coating. It was clearly demonstrated that the oxidation process considerably improved the surface strength of the coating, indicating that oxidation was accompanied by annealing of the coating structure, which would result in the release of residual stresses and hence affect the adhesion between the coating and Mg alloy, resulting in much better wear resistance.



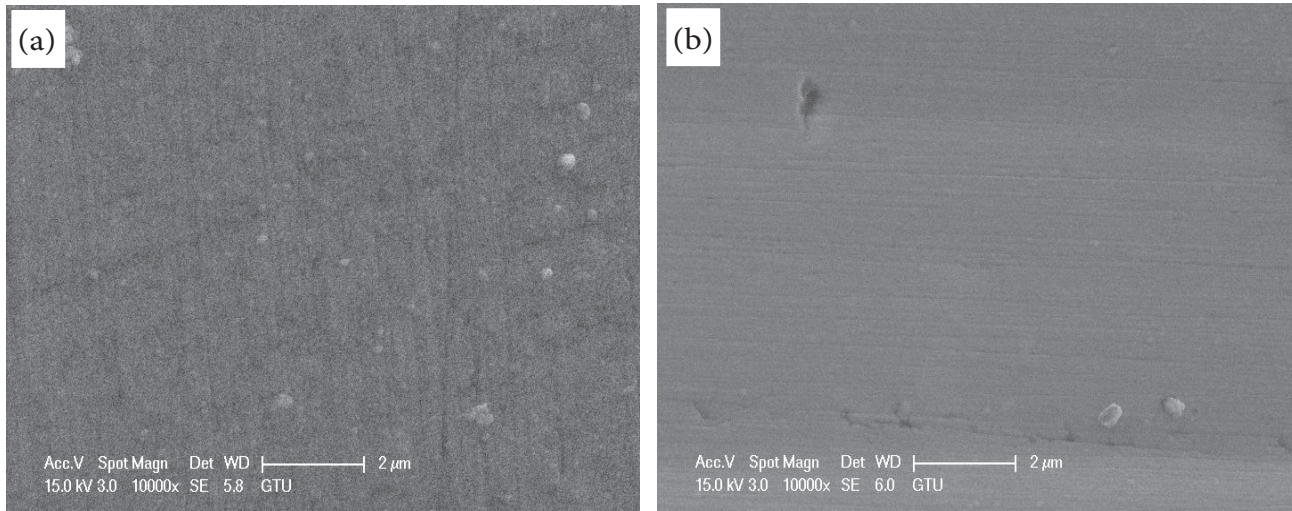
**Figure 2.** Scanning electron micrographs of 6-mm scratches produced on 11 layers TiVN/VN coatings (a) before oxidation and (b) after oxidation by means of a Rockwell scratch test under a stepwise process increasing up to a final load of 2 N at low magnification. (c) and (d) show the high magnification of respective images.

Figure 3 demonstrates the variation of friction coefficient with respect to normal load for both films recorded during the scratching. For both films, the initial value of the coefficient of friction is approximately 0.15; however, as the load progressively increased and delamination of the coating occurred, the coefficient of friction increased continuously due to the inclusion of trapped wear particles at the interface. The coefficient of friction suddenly increased after the normal load of 0.9 N and reached the value of the friction coefficient of AZ91D Mg alloy, indicating that the coating completely lifted off from the surface and the diamond tip reached the substrate. However, the coefficient of friction for the oxidized film showed a gradual increase and the maximum value of the coefficient of friction reached at the end of the test is lower than that for the unoxidized coating. The lower coefficient of friction after the oxidation process can be associated with the lubricious oxide layer forming on the surface. Figure 4 shows the SEM images of TiVN/VN multilayer film coatings before and after the oxidation process. While the unoxidized multilayer film looks rather rough, the oxidized film surface is quite smooth. As obtained from the low coefficient of friction, the lubricious oxide layer led to the smoother surface. Similarly, RMS values obtained from AFM images are 4.5 nm and 2.6 nm for unoxidized and oxidized coatings, respectively. This indicates that the oxidation process leads to a smoother surface; the  $V_2O_5$  layer formed on the multilayer coating during this process protects the surface against wear.

Figure 5 depicts the nanohardness and elastic modulus of TiVN/VN multilayer coatings. While the hardness value of pure AZ91D Mg-alloy materials is 74 HV, this value increased approximately 15 times after performing TiVN/VN [28]. The hardness values of the as-grown and oxidized 11 layers TiVN/VN coatings were 1029 and 1160 HV, respectively, while the elastic modulus values of as-grown and oxidized TiVN/VN multilayer coatings were 89 and 96 GPa, respectively. The increase in hardness and elastic modulus after oxidation process is clearly related to the hardening effect of the oxidization process. Coating hardness can be affected by density,



**Figure 3.** Load-dependent friction coefficient of oxidized and unoxidized TiVN/VN coatings.



**Figure 4.** SEM images of 11 layers TiVN/VN coatings (a) before and (b) after oxidation process.

morphology, stoichiometry, and grain size. Although the low-temperature annealing process was applied under partial oxygen pressure, heat treatment might have affected the interlayer interaction and resulted in the release of stresses between each layer. It is also possible that oxygen atoms were diffused into the coating during the oxidation process, leading to smaller grain size, which resulted in higher hardness.

In order to investigate the oxygen diffusion mechanism, we have developed TiVN/VN multilayer coatings composed of 5, 11, and 33 alternating layers of TiVN and VN. The coatings were made with varying numbers of layers by keeping the same total coating thickness of 660 nm. Their surfaces were then oxidized under the same conditions and the mechanical properties of these coatings were investigated. The hardness values of oxidized 5-, 11-, and 33-layer coatings were 1665, 1160, and 365 HV, respectively. As can be seen in the inset of Figure 5, the load-displacement curves of 5- and 11-layer coatings of oxidized TiVN/VN demonstrated a similar trend. The maximum penetration depth of a 5-layer coating was slightly lower due to the improvement of interlayer shear stress with a decreasing modulation period. Moreover, as it had the thickest VN layer on the top surface,

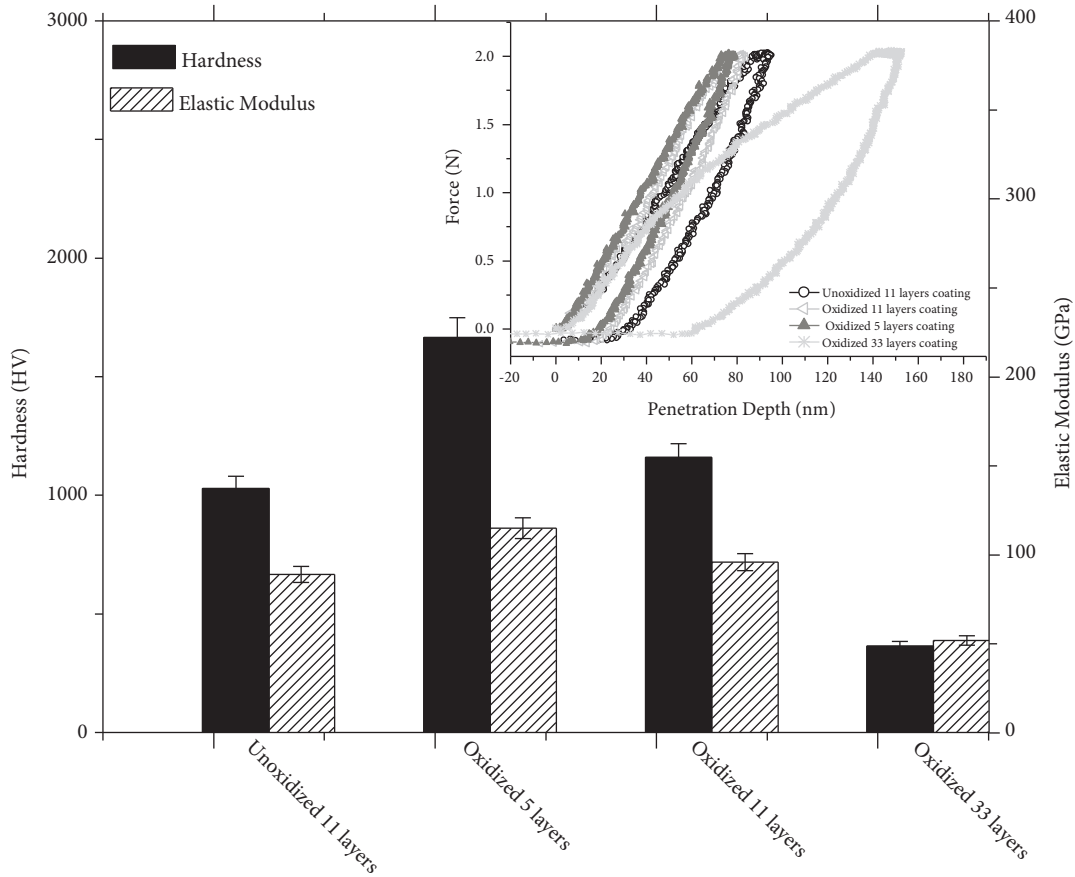


**Figure 5.** Hardness and elastic modulus values of TiVN/VN coatings with a variable layer period. The inset shows the load–unload curves for TiVN/VN multilayer coatings with various periods obtained with nanoindentation using a constant applied force.

oxidized 5-layer TiVN/VN coating demonstrated the least amount of deformation, attributed to the lubricious oxide layer providing less molecular movement under constant load. However, the load-displacement curve of 33 layers of TiVN/VN coating displayed a dramatic increase in penetration far exceeding those of the other coatings; it exhibited behavior expected from a brittle material, so that the recovery curve of the films during the unloading process has 2 different slopes. The greater penetration and low elastic modulus are indicative of a soft structure for the coating. Increasing the number of interfaces generated a higher degree of plastic deformation in the coatings due to the inhibition of dislocation motion by alternating layer lattice strain.

The effect of layer periodicity and subsequent oxidation on the wear properties of TiVN/VN multilayer coatings was also investigated. As a result of scratch tests,  $L_{c1}$  values, where the first fractions occurred with increasing applied load, were determined as 780, 660, and 610 mN for 5-, 11-, and 33-layer coatings, respectively. As the number of layers was reduced, the wear properties improved due to the decrease in internal and residual stresses. When layers were formed, bond stresses occurred between atoms due to crystal structure mismatch at the interface. When the thickness of the layers reached the ideal thickness, the defects arising from the stresses were minimized.

#### 4. Conclusion

The goal of this work was to characterize TiVN/VN multilayer coatings deposited by magnetron sputtering and to determine the influence of surface oxide layer formation under UHV conditions on their morphology and mechanical properties, including structure, wear, and hardness. The oxidized TiVN/VN multilayer coatings exhibited better adhesion and lower friction coefficient associated with the decrease of the RMS roughness and the formation of a self-lubricating  $V_2O_5$  layer on the coating surface. As the thickness of the top VN layer increased, wear properties of the coatings were improved. The improvement in the hardness of the oxidized coating is associated with the release of stresses between each layer after in-situ annealing.

#### 5. Acknowledgments

The authors would like to acknowledge the funding of this work by the Scientific and Technological Research Council of Turkey (TÜBİTAK, Project No: 113M134). In addition, the authors would like to thank Assistant Professor Fevzi Çakmak Cebeci for his assistance.

#### References

- [1] Braic M, Balaceanu M, Braic V, Vladescu A, Pavelescu G, Albulescu M. *Surface and Coatings Technology* 2005, 200, 1014-1017.
- [2] Hübler R, Schröer A, Ensinger W, Wolf G, Schreiner W, Baumvol I. *Surface and Coatings Technology* 1993, 60, 561-565.
- [3] Leng Y, Sun H, Yang P, Chen J, Wang J, Wan G, Huang N, Tian X, Wang L, Chu P. *Thin Solid Films* 2001, 398, 471-475.
- [4] Hübler R, Cozza A, Marcondes T, Souza R, Fiori F. *Surface and Coatings Technology* 2001, 142, 1078-1083.
- [5] Chim YC, Ding XZ, Zeng XT, Zhang S. *Thin Solid Films* 2009, 517, 4845-4849.
- [6] Rainforth WM, Zhou Z. *J Phys Conf Ser* 2006, 26, 89-94.
- [7] Barshilia HC, Rajam KS. *Bulletin of Materials Science* 2003, 26, 233-237.
- [8] Qiu YX, Zhang S, Li B, Wang YX, Lee JW, Li FJ, Zhao DL. *Surf Coat Tech* 2013, 231, 357-363.
- [9] Helmersson U, Todorova S, Barnett SA, Sundgren JE, Markert LC, Greene JE. *J Appl Phys* 1987, 62, 481-484.
- [10] Ananthakumar R, Subramanian B, Kobayashi A, Jayachandran M. *Ceram Int* 2012, 38, 477-485.
- [11] Uslu ME, One AC, Ekinici G, Toydemir B, Durdu S, Usta M, Arslan LC. *Surf Coat Tech* 2015, 284, 252-257.
- [12] Kong M, Shao N, Dong YS, Yue HL, Li GY. *Mater Lett* 2006, 60, 874-877.
- [13] Luo Q, Zhou Z, Rainforth WM, Hovsepian PE. *Tribol Lett* 2006, 24, 171-178.
- [14] Fateh, N.; Fontalvo, G. A.; Gassner, G.; Mitterer, C. *Wear* 2007, 262, 1152-1158.
- [15] Gassner G, Mayrhofer PH, Kutschej K, Mitterer C, Kathrein M. *Tribol Lett* 2004, 17, 751-756.
- [16] Franz R, Mitterer C. *Surface & Coatings Technology* 2013, 228, 1-13.
- [17] Aouadi SM, Gao H, Martini A, Scharf TW, Muratore C. *Surface & Coatings Technology* 2014, 257, 266-277.
- [18] Fateh N, Fontalvo GA, Gassner G, Mitterer C. *Tribol Lett* 2007, 28, 1-7.
- [19] Glaser A, Surnev S, Netzer FP, Fateh N, Fontalvo GA, Mitterer C. *Surf Sci* 2007, 601, 1153-1159.
- [20] Fateh N, Fontalvo, GA, Mitterer C. *Tribol Lett* 2008, 30, 21-26.
- [21] Sanjines R, Wiemer C, Hones P, Levy F. *J Appl Phys* 1998, 83, 1396-1402.
- [22] Subramanian B, Ananthakumar R, Kobayashi A, Jayachandran M. *Journal of Materials Science-Materials in Medicine* 2012, 23, 329-338.
- [23] Demeter M, Neumann M, Reichelt W. *Surf Sci* 2000, 454, 41-44.



- [24] Silversmit G, Depla D, Poelman H, Marin GB, De Gryse R. *J Electron Spectrosc* 2004, 135, 167-175.
- [25] Fateh N, Fontalvo GA, Mitterer C. *J Phys D Appl Phys* 2007, 40, 7716-7719.
- [26] Tillmann W, Sprute T, Hoffmann F, Chang YY, Tsai CY. *Surface & Coatings Technology* 2013, 231, 122-125.
- [27] Kutschej K, Mayrhofer PH, Kathrein M, Polcik P, Mitterer C. *Surface & Coatings Technology* 2005, 200, 1731-1737.
- [28] Lee WB, Kim JW, Yeon YM, Jung SB. *Mater Trans* 2003, 44, 917-923.